A 2-D ORIENTATION ADAPTIVE PREDICTION FILTER IN LIFTING STRUCTURES FOR IMAGE CODING [1]

Ömer N. Gerek[1] *and A. Enis Çetin*[2]

[1]Anadolu University, Department of Electrical and Electronics Eng.,

Eskişehir TR-26470, Turkey

E-mail: ongerek@anadolu.edu.tr

[2]Bilkent University, Dept. of Electrical Engineering,

Bilkent, Ankara TR-06533, Turkey

Abstract

Lifting-style implementations of particular wavelets are popular in image coders. We present a 2–D extension and modification to the prediction part of the lifting implementation type Daubechies 5/3 wavelet. The 2–D prediction filter predicts the value of the next polyphase component according to an edge orientation estimator of the image. Consequently, the prediction domain is allowed to rotate + or − 45 degrees in regions with diagonal gradient. The proposed structure can be implemented in horizontal and vertical directions similar to a 1–D lifting applied to an image. The gradient estimator was inspired from a method to interpolate missing color sensor values in CCD arrays of image sensors, which is computationally inexpensive with additional costs of only 6 subtractions per lifting instruction, and no multiplications are required. We have observed plausible coding results with conventional wavelet encoders.

I. Introduction

The 5/3 Daubechies biorthogonal wavelet has received a wide range of interest in various applications due to its filter tap coefficients which are particularly useful in real-time implementations. Furthermore, the lifting implementation of this wavelet contains filters with coefficients that can be written as powers of two leading to a multiplication free realization of the filter-bank [1], [2]. Several linear or nonlinear decomposition structures that are published in the literature report better performance than the 5/3 wavelet using signal adapted filters including [2]–[7]. Among these works, [2] shows the method to achieve the lifting style implementation of any DWT filter bank, whereas [3] extends the idea of linear filters in the lifting style to nonlinear filters. In [4], [8], and [7], the lifting prediction filter was made adaptive according to the local signal properties, and in [6], the importance of coder–nonlinear transform strategy was emphasized. The idea of lifting adaptation was also applied to video processing [9], [10]. Finally, in [5], [11], and [12], 2–D extensions of the lifting structures were examined, which fundamentally resembles the idea of this work. Nevertheless, the 5/3 wavelet has an efficient set of filter coefficients which enables fast, simple, and integer-shifts-only implementations, and due to these properties, it was also adopted by the JPEG-2000 image coding standard [13], [14] in its lossless mode.

[1]A. E. Cetin's work is partially funded by TUBITAK and TUBA (Turkish Academy of Sciences) GEBIP Programme, and O. N. Gerek's work is supported by Anadolu University Research Fund under Contract No. 030263.

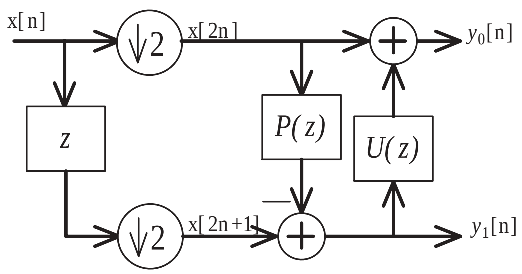

Fig. 1. *Lifting analysis stage.*

The 5/3 wavelet has an efficient set of filter coefficients which consist of simple integer fractions: $h_0 = [-1/8, 1/4, 3/4, 1/4, -1/8]$ and $h_1 = [-1/2, 1, -1/2]$. Its lifting implementation is even more efficient and can be realized using binary shifting operations as follows:

$$
\begin{aligned}
y_1[n] &= x[2n+1] - \frac{1}{2}\left(x[2n] + x[2n+2]\right) \\
y_0[n] &= x[2n] + \frac{1}{4}\left(y_1[n-1] + y_1[n]\right) \\
&= -\frac{1}{8}x[2n-2] + \frac{1}{4}x[2n-1] + \frac{3}{4}x[2n] + \frac{1}{4}x[2n+1] - \frac{1}{8}x[2n+2]
\end{aligned} \tag{1}
$$

where $x[n]$ is the input signal, $y_1[n]$ is the high–pass detail signal, and $y_0[n]$ is the low–pass approximation signal. Notice that prediction filter is very short, consisting of an averaging operation performed over the left and right neighboring samples in a row (or column) in two-dimensional image processing. The lifting structure corresponding to Eq. 2 is shown in Figure 1.

The above lifting implementation is purely one dimensional. In other words, the image is processed line by line during implementation. In two-dimensional separable extension of the above filterbank the image is first processed horizontally (or vertically) and then processed vertically (or horizontally) to obtain four subband images. Let us consider the row–wise processing of an image $x[m, n]$. The prediction filter inherently assumes that the right and left neighbor pixels are closely related with the pixels between them. As a result, $(x[m, 2n] + x[m, 2n+2])/2$ will be an accurate estimate of $x[m, 2n+1]$. Hence, by subtracting this prediction estimate from the true value of $x[m, 2n+1]$, a small residue is obtained. This residual signal corresponds to the detail signal obtained after the single stage wavelet transformation. This may not be a good strategy around a vertical or a diagonal edge because $x[m, 2n]$ may be unrelated to $x[m, 2n+2]$. On the other hand, some of the four other immediate diagonal neighbors $x[m+1, 2n+2]$, $x[m+1, 2n-2]$, $x[m-1, 2n+2]$ and $x[m-1, 2n-2]$ of $x[m, 2n+1]$ may be closer to the pixel $x[m, 2n+1]$ in value. Therefore, it may be better to use two of these four diagonal neighbors in the prediction stage of the lifting structure in a judicious manner. Our adaptive predictor is obtained by relaxing the condition that the predictor should use samples from the current row that it is processing. In the next section, a computationally

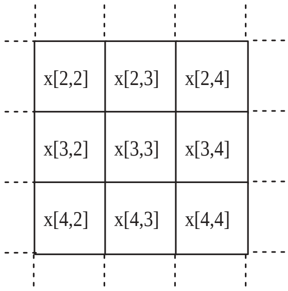

Fig. 2. *A 3 by 3 pixel array.*

efficient adaptation strategy describing how to switch from single-line horizontal processing to multi-line horizontal processing is presented. The predictor can still use only two pixels for computational efficiency as in [1], however it can select them from the neighboring rows instead of the current row. Resultant lifting scheme can still be implemented in two stages consisting of a row-wise processing followed by a column-wise processing as in ordinary lifting.

The proposed analysis filterbank does neither require any multiplications nor transmission of any side information during implementation. Due to its locally adaptive nature, this work may be categorized in a class of works reported in [8]-[12]. It was also reported in [11] that such multi–line lifting realizations can be performed in a memory–efficient manner.

II. Edge Sensitive Adaptive Prediction

Our aim is to develop a multiplierless edge sensitive predictor that can be used in the prediction stage of the lifting structure. A multiplierless edge sensing interpolator [15] is used in missing color pixel interpolation in CCD imaging systems. Let us try to estimate the pixel $x[3,3]$ shown in Figure 2 using its immediate neighbors. The adaptive interpolation algorithm is based on the following principles:

- If the up and down pixel value difference is less than the left and right pixel value difference, then the interpolation value is (up + down)/2,
- else estimate the missing pixel $x[3,3]$ using its left and right neighbors (left + right)/2.

Let us first define horizontal and vertical differences in terms of samples in Figure 2:

$$\begin{aligned} \Delta_h &= |x[3,2] - x[3,4]| \\ \Delta_v &= |x[2,3] - x[4,3]| \end{aligned}$$

The estimated value of $x[3,3]$ is determined as follows

$$\hat{x}[3,3] = \begin{cases} (x[3,2]+x[3,4])/2 & , \; if \Delta_h < T \text{ and } \Delta_v > T \\ (x[2,3]+x[4,3])/2 & , \; if \Delta_h > T \text{ and } \Delta_v < T \\ (x[2,3]+x[3,2]+x[3,4]+x[4,3])/4 & , \; otherwise. \end{cases} \quad (2)$$

If there is a vertical (horizontal) edge going through pixel $x[3,3]$ then horizontal (vertical) pixels are used in interpolation. Otherwise, the four nearest neighbors of $x[3,3]$ are used. In this way, the missing pixel value is approximated according to the most likely gradient of the image around $x[3,3]$. This interpolation strategy gives a good approximation of a possibly missing color sensor output, so it improves both the mean-square-error and the subjective quality of the acquired color image in CCD imaging systems.

In this paper, a similar interpolation scheme is developed in the prediction part of a lifting stage in image processing. The predictor does not have to be limited to use samples from the same row (or column in columnwise processing). In ordinary lifting implementation, the available polyphase samples are horizontally down-sampled pixels of the image, such as $x[m,2n-2]$, $x[m,2n]$, $x[m,2n+2]$, etc. while processing the image along the rows. For the prediction of a particular pixel value, say $x[m,2n+1]$, none of the samples from the upper and lower columns are included in the domain of prediction during row-wise processing in an ordinary lifting structure. On the other hand, the column to the left and to the right are *completely* available for prediction in many image and video processing applications.

In this work, we allow the use of appropriate polyphase pixels from the rows above and below the pixel of interest for the prediction part of the lifting stage. In row–wise processing, the ordinary 5/3 biorthogonal wavelet lifting structure uses $1/2\,(x[m,2n]+x[m,2n+2])$ for predicting the value of $x[m,2n+1]$. We introduce four more diagonal neighboring samples from the upper and lower rows. For example, $x[m,2n+1]$ may also be predicted using

- $1/2\,(x[m-1,2n]+x[m+1,2n+2])$ which corresponds to the average of the north–west neighbor and the south–east neighbor, or
- $1/2\,(x[m+1,2n]+x[m-1,2n+2])$ which corresponds to the the average of north–east neighbor and the south–west neighbor.

As an example, if the local gradient is in the south-east direction, then there is more possibility that the center of the 3×3 region has a pixel value similar to its north-east and south-west neighbors, which are in a direction orthogonal to the gradient. This concept is generalized to the other directions according to the following adaptation rule for the selection of prediction domain pixels. Let us first define: $\Delta_{135} = |x[m-1,2n]-x[m+1,2n+2]|$, $\Delta_0 = |x[m,2n]-x[m,2n+2]|$, $\Delta_{45} = |x[m+1,2n]-x[m-1,2n+2]|$ as absolute differences between some of the

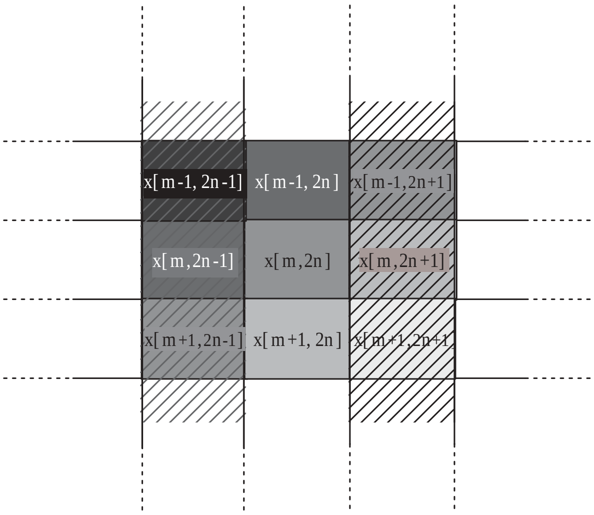

Fig. 3. *A sample image segment with south–east gradient.*

neighbors of the pixel $x[m, 2n+1]$.

- If Δ_{135} is the least among Δ_{135}, Δ_0, and Δ_{45}, then the prediction estimate is given by:

$\hat{x}[m, 2n+1] = (x[m-1, 2n] + x[m+1, 2n+2])/2$

- If Δ_0 is the least among Δ_{135}, Δ_0, and Δ_{45}, then the prediction estimate is given by:

$\hat{x}[m, 2n+1] = (x[m, 2n] + x[m, 2n+2])/2$

- If Δ_{45} is the least among Δ_{135}, Δ_0, and Δ_{45}, then the prediction estimate is given by:

$\hat{x}[m, 2n+1] = (x[m+1, 2n] + x[m-1, 2n+2])/2$

In the example shown in Figure 3, the largest gradient is in the south-east direction. As a result, Δ_{45} is the minimum difference. Therefore, the value of $x[m, 2n]$ must be predicted as $(x[m-1, 2n+1] + x[m+1, 2n-1])/2$. It must be noted that such a *tilted* prediction ($P(\mathbf{z})$) does not require transmission of any side information, because the pixels used in prediction and the pixel to be predicted belong to different polyphase components. In Figure 3, the dashed pixels constitute the prediction domain for predicting $x[m, 2n]$ during horizontal process. In case of no quantization, these columns are automatically reconstructed and the decoder uses the *same* directional choice method that was used in encoder.

Since the the immediate two vertical neighbors ($x[m-1, 2n]$ and $x[m+1, 2n]$) coincides with the same polyphase domain of $x[m, 2n]$, they cannot be used for predicting the value of $x[m, 2n]$ in a lifting structure. Therefore, edges that are perpendicular to the process direction cannot be interpolated as efficiently as diagonal edges. But this limitation is inherent in progressive horizontal and vertical wavelet processing of images.

In one-dimensional single-line processing, the subsignals $y_0[n]$ and $y_1[n]$, are related to even $x_e[n]$ and odd $x_o[n]$ components of the signal $x[n]$ via the relation

$$\begin{bmatrix} Y_0(z) \\ Y_1(z) \end{bmatrix} = \begin{bmatrix} 1-P(z)U(z) & U(z) \\ -P(z) & 1 \end{bmatrix} \begin{bmatrix} X_e(z) \\ X_o(z) \end{bmatrix} \tag{3}$$

If the lifting implementation is carried out using ordinary single-line processing, the polyphase transform matrix takes the following form in the z-domain:

$$\begin{bmatrix} 1-\frac{1}{8}(1+z)(1+z^{-1}) & \frac{1}{4}(1+z^{-1}) \\ -\frac{1}{2}(1+z) & 1 \end{bmatrix} \tag{4}$$

This matrix provides the coefficient information to generate the analysis filters in a filter–bank structure:

$$\begin{bmatrix} H_{0,ev}(z) & H_{0,odd}(z) \\ H_{1,ev}(z) & H_{1,odd}(z) \end{bmatrix} \tag{5}$$

and $H_i(z) = H_{i,ev}(z^2) + z^{-1}H_{i,odd}(z^2)$, for $i = 0, 1$. Considering a 2–D signal, if multi-line processing is performed, the delay elements z_1^{-1} and z_2^{-1}, which correspond to vertical and horizontal directions, must be used simultaneously. For example, for the south-west - to - north-east prediction direction, the polyphase matrix becomes:

$$\begin{bmatrix} 1-\frac{1}{8}(z_1^{-1}+z_1\cdot z_2)(1+z_2^{-1}) & \frac{1}{4}(1+z_2^{-1}) \\ -\frac{1}{2}(z_1^{-1}+z_1\cdot z_2) & 1 \end{bmatrix} \tag{6}$$

The low–pass and high–pass filters of the filter–bank corresponding to the matrix in (6) are directional two-dimensional (2-D) filters in the spatial–domain.

Considering the horizontal process of the image, a drawback of the above adaptive lifting structure is that the approximation coefficient $y_0[m,n]$ is generated from polyphase samples ($x[m,2n+1]$) that are predicted from *other* rows' polyphase samples ($x[m+1,2n]$ and $x[m-1,2n]$). Therefore, there is a row–wise lifting update leakage. Because of this leakage, the effect of $\mathbf{U(z)}$ in the lifting stage deviates from anti–aliasing low pass filter. This situation leads to distortions in low-low subimages across decomposition scales. This problem can be solved by changing the order of the update $U(z)$ and the prediction $P(z)$ stages of Figure 1 as discussed in the next section. With the proper choice of the low–pass filter, the new $U(z)$ can be performed prior to the prediction, and its implementation still requires no multiplications, so the computational efficiency is retained.

III. Adaptive Lifting Structure Performing Low-pass filtering First

High quality low-low images can be obtained by performing low-pass filtering first in a lifting structure. A half-band low-pass filter can be put into an isolated update lifting stage as in [4].

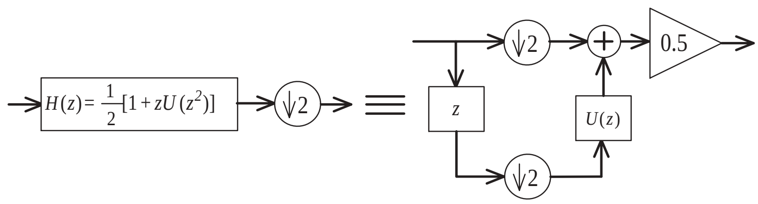

Fig. 4. *Lifting update implementation of a half–band filter.*

In order to achieve a multiplierless structure we consider the simple Lagrangian half–band low-pass filter: $\mathbf{h}_3 = \{1/4, 1/2, 1/4\}$. The z-transform of this filter is

$$H(z) = \frac{1}{2}(1 + z(U(z^2)) \quad (7)$$

where $U(z) = \frac{1}{2}z^{-1} + \frac{1}{2}$. This low-pass filter followed by down sampling can be implemented in a lifting structure due to the relation known as Noble-Identity. The resulting structure is shown in Figure 4. The filter $U(z)$ corresponding to $\mathbf{h}_3$ is $U(z) = \frac{1}{2}z^{-1} + \frac{1}{2}$. This is a very simple update filter which can be implemented by a single summation and a division by two, which is one bit shift–right.

After this stage, adaptive prediction algorithm described in previous region can be implemented. Since the low-pass filtering is performed first, the low-low subimages are as good as those obtained by any sub-band decomposition structure using the third-order Lagrange half-band filter.

The overall structure including the low–pass filter is still computationally comparable to the original implementation of the Daubechies 5/3 wavelet in terms of calculations per lifting operation.

IV. Experimental Results and Conclusions

The selection of prediction domain in the lifting stage has a number of practical advantages. We have experimentally observed that, in a typical test image, among $1/2\,(x[m-1, 2n] + x[m+1, 2n+2])$, $1/2\,(x[m, 2n] + x[m, 2n+2])$, and $1/2\,(x[m+1, 2n] + x[m-1, 2n+2])$, the possibility of the horizontal process $(1/2\,(x[m, 2n] + x[m, 2n+2]))$ being the best prediction of $x[m, 2n+1]$ is 30.1 %. This is slightly less than about one–thirds of the possible predictions. As a result, persistently using horizontal prediction loses chances of making better prediction decisions. On the other hand, our directionally sensitive prediction decision rule catches about 52 % of the best predictions as described above. This improvement reflects to practical compression results, too.

In the absence of quantization, perfect reconstruction of the proposed algorithm is assured due to the symmetric lifting implementations. On the other hand, the choice of minimum Δ_{135}, Δ_0, and Δ_{45} has a chance to alter if the transform coefficients are quantized. However, it is experimentally observed that this does not occur with wavelet tree bitplane coders at compression ratios down to 0.5 bpp for 8 bpp originals. Below this bit rate, the orientation

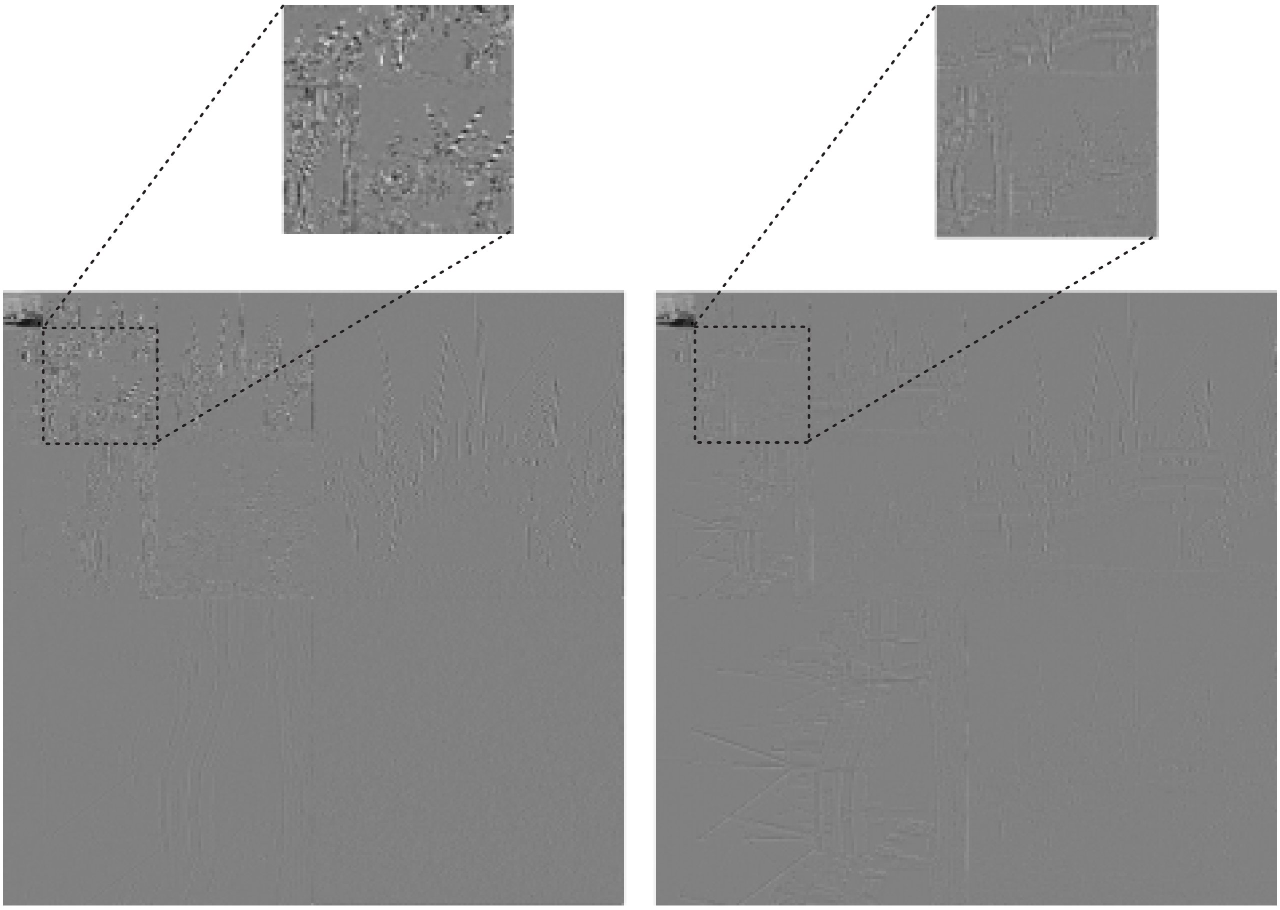

(a) (b)

Fig. 5. *Wavelet trees obtained by (a) regular 5/3 wavelet, (b) our method.*

selection rule of the decoder starts to deviate from that of the encoder at arbitrary image locations. This shows that the direction adaptation rule is fairly robust to fine quantization, and the proposed method is suitable for relatively high bit rate compression.

In Figure 5, (a) original 5/3 wavelet decomposition, and (b) directionally modified prediction lifting decomposition images of one of the test images are shown respectively. Notice that the detail images obtained by the directionally adaptive 5/3 wavelet exhibits less signal energy at several decomposition levels in general. In this example, the high pass coefficients in Figure 5(a) have a variance = 94.06, and a sample entropy = 3.4536, whereas the high pass coefficients in 5(b) have variance = 30.57, and sample entropy = 3.4412. This behavior is observed in other test images, as well. The energy reduction shows that better compression results can be obtained using our method, as compared to the 5/3 wavelet in high-band subimages.

For presenting practical results, a bitplane compression method [13], [14] is used to encode the transform domain coefficients. A decomposition level of 4 was selected for 512×512 images. The PSNR values for a set of test images at 1 bpp and 0.5 bpp are shown in Table I for our directionally adaptive method using the half-band anti-aliasing update filter and 5/3 Daubechies wavelet. The same encoder is used in both cases. In general, plausible PSNRs are obtained for a given compression level in our filterbank.

	Orig. 5/3 at 1bpp	Our method at 1bpp	Orig. 5/3 at 0.5bpp	Our method at 0.5bpp
boats ($\sigma^2 = 2466$,I= 7.03)	37.04	37.20	33.30	33.33
airfield ($\sigma^2 = 3594$,I= 7.12)	28.48	29.01	26.70	26.81
bridge ($\sigma^2 = 2996$,I= 5.71)	27.93	28.00	25.61	25.59
harbor ($\sigma^2 = 1565$,I= 6.76)	32.40	32.58	28.14	28.20
lena ($\sigma^2 = 2290$,I= 7.44)	37.11	37.10	33.75	33.69
barbara ($\sigma^2 = 2982$,I= 7.63)	32.70	32.68	28.21	28.13
houses ($\sigma^2 = 2423$,I= 7.48)	33.48	33.61	31.14	31.19
garden ($\sigma^2 = 5665$,I= 7.52)	31.47	31.69	24.22	24.42
topkapi ($\sigma^2 = 6314$,I= 7.28)	34.24	34.35	29.29	29.35
duomo ($\sigma^2 = 1256$,I= 6.92)	28.08	28.21	24.85	24.93
peppers ($\sigma^2 = 2894$,I= 7.59)	35.65	35.71	33.20	33.21

TABLE I

Experimental results for 512×512 test images (sample variance = σ^2 and sample entropy = I) at 1 bpp and 0.5 bpp.

The proposed method better preserves sharp edges of the original image compared to the ordinary 5/3 wavelet decomposition. This is because of the reduced high-band signal energy at edge locations compared to the 5/3 wavelet decomposition. The following example illustrates the visual improvement obtained by our method. The test image is listed as "garden" in Table 1 contains printed text on a natural flower background. Small portions of images from 0.5 bpp coded versions of this image are shown in Figure 6. Figure 6(a) shows the regular 5/3 wavelet coded version, and Figure 6(b) shows the result from our method. Edges are sharper with less ringing artifacts in Figure 6(b). This is because, in general, our lifting strategy provides better prediction around diagonal edges of the original image.

In spite of the edge adaptation of the prediction, the overall proposed method gives marginally better or similar PSNR values as compared to the 5/3 wavelet. The reason for this situation is due to the low–pass filtering prior to the prediction. This filter automatically reduces some amount of prediction information in the upper polyphase component. We have observed that a combination of the given low–pass filter followed by a 1D prediction filter (as used in the 5/3 wavelet) gives worse PSNR results than the original 5/3 wavelet. By incorporating the 2–D orientation adaptations, the PSNR results improve to better than or comparable with the 5/3 wavelet. On the other hand, the use of the low–pass filter in the upper polyphase is essential because without this filter, the downsampling process yields aliased ll images which are harder to process in the later decomposition stages.

The computational complexity of the proposed adaptive filterbank is very low. Our directionally adaptive lifting

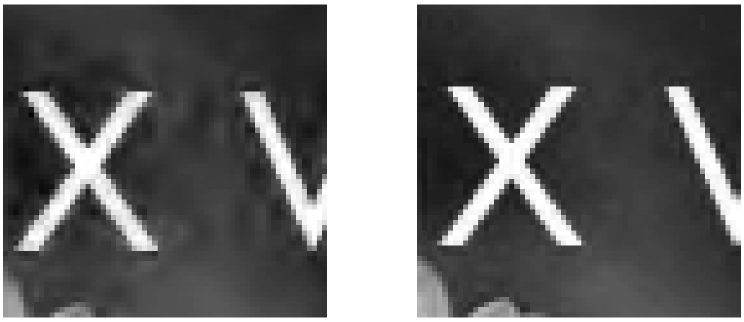

(a) (b)

Fig. 6. *A detail from "garden" image coded at 0.5 bpp using (a) the 5/3 wavelet, and (b) our method.*

strategy contains an additional

1. three difference operations to obtain Δ_{135}, Δ_0, and Δ_{45}, and
2. three comparison operations to choose the minimum of Δ_{135}, Δ_0, and Δ_{45}

compared to Daubechies 5/3 wavelet decomposition.

The rest of the operations, including the anti–aliasing filtering have identical complexity figures as the original 5/3 lifting implementation. The above operations can be summarized as an additional complexity of 6 subtractions per lifting (including prediction and update) operation. For an $N \times N$ image, there are approximately N^2 lifting operations, so the additional computational cost is $6N^2$ subtractions. There is neither any integer nor floating point multiplications in the new structure. As a result, our directionally adaptive algorithm keeps the low complexity property of the 5/3 Daubechies wavelet decomposition, and provides plausible image compression results for all the test images that are tried at bitrates above 0.5 bpp.

References

[1] Wim Sweldens, "The Lifting Scheme: A new philosophy in biorthogonal wavelet constructions," In A. F. Laine and M. Unser, editors, *Wavelet Applications in Signal and Image Processing III*, pp. 68-79, Proc. SPIE 2569, 1995.

[2] Ingrid Daubechies and Wim Sweldens, "Factoring Wavelet Transforms into Lifting Steps," *Journal of Fourier Analysis and Appl.*, Vol. 4, Nr. 3, pp. 247-269, 1998.

[3] R. L. Claypoole, G. M. Davis, W. Sweldens W, et al. "Nonlinear wavelet transforms for image coding via lifting,"*IEEE Trans. on Image Processing,* Vol. 12, No. 12, pp.1449–1459, Dec. 2003.

[4] Ö. N. Gerek and A. E. Çetin, "Adaptive Polyphase Subband Decomposition Structures for Image Compression," *IEEE Trans. on Image Processing,* Vol. 9, No. 10, pp.1649–1660, Oct. 2000.

[5] A. Gouze, M. Antonini, M. Barlaud, and B. Mack, "Design of signal–adapted multidimensional lifting scheme for lossy coding," *IEEE Trans. on Image Processing,* to appear, Dec. 2004.

[6] A. Cohen, I. Daubechies, O. G. Guleryuz, and M. T. Orchard, "On the importance of combining wavelet-based nonlinear approximation with coding strategies," *IEEE Trans. Inform. Theory,* 48(7):1895–1921, 2002.

[7] T. Chan and H. M. Zhou, "Adaptive ENO–Wavelet Transforms for Discontinuous Functions," UCLA Report No. CAM 99-21, June 1999.

[8] G. Piella, B. Pesquet-Popescu, H. Heijmans , “Adaptive update lifting with a decision rule based on derivative filters,” *IEEE Signal Processing Letters,* pp. 329- 332, Oct. 2002.

[9] G. Pau, C. Tillier, B. Pesquet-Popescu, “Optimization of the Predict Operator in Lifting-Based Motion Compensated Temporal Filtering,” *SPIE VCIP,* San Jose, CA, Jan. 2004.

[10] N. Mehrseresht and D. Taubman, “Adaptively weighted update steps in motion compensated lifting based on scalable video compression,” Proc. IEEE International Conference on Image Processing (ICIP), volume 2, pp. 771-774, Sep. 2003.

[11] D. Taubman, “Adaptive, non-separable lifting transforms for image compression,” Proc. IEEE International Conference on Image Processing (ICIP), volume 3, pages 772-776, Oct. 1999.

[12] H. Heijmans, G. Piella, B. Pesquet-Popescu, “Building Adaptive 2D Wavelet Decompositions by Update Lifting”, *Proc. of IEEE Int. Conf. on Image Proc.,* Rochester, Oct. 2002.

[13] I. J. S. WG01, “JPEG-2000 part-1 standard,” ISO/IEC 15444-1.

[14] C. Christopoulos, A. Skodras, and T. Ebrahimi, “The JPEG2000 still image coding system: An overview,” *IEEE Transactions on Consumer Electronics,* Vol. 46, No. 4, pp. 11031127, Nov. 2000.

[15] Robert H. Hibbard, “Apparatus and method for adaptively interpolating a full color image utilizing luminance gradients,” U.S. Patent 5,382,976.